Intramolecular Vibrational Energy Redistribution Involving the Torsion in CF_3CH_3: A Molecular Dynamics Study†

Philip J. Stimac‡ and John R. Barker*,‡,§

Department of Atmospheric, Oceanic, and Space Sciences, University of Michigan, Ann Arbor, Michigan 48109-2143, and Department of Chemistry, University of Michigan, Ann Arbor, Michigan 48109-1055

Received: November 23, 2005; In Final Form: January 13, 2006

Classical trajectory calculations on intramolecular vibrational energy redistribution (IVR) involving the torsion in 1,1,1-trifluoroethane (TFE) are reported. Two potential energy functions (PEFs) are used to describe the potential energy surface. The "full" PEF gives excellent agreement with the experimental vibrational frequencies. The "simple" PEF omits nondiagonal interaction terms, but still gives very good agreement with the experimental frequencies. The "simple" PEF is intended to minimize mode−mode coupling. Neither PEF includes the HF elimination reaction. Calculations are carried out both with nominal microcanonical selection of initial coordinates and momenta, and with a modified selection method that places controlled amounts of energy in the torsion. Total (classical) vibrational energies from 0.005 to 140 kcal mol^{-1} are investigated. The calculated time constants describing energy flow out of the torsional mode are <10 ps for classical vibrational energies near the classical reaction threshold energy (~75 kcal mol^{-1}) and greater. It is found that the rate of decay from the torsion largely depends on the amount of energy in the other vibrational modes. Analysis using power spectra shows that the torsional mode in TFE is strongly coupled to the other vibrational modes. These results strongly suggest that vibrational energy in TFE will not be sequestered in the torsion for time periods greater than a few tens of picoseconds when the molecule has enough energy to react via HF elimination.

I. Introduction

Recently, Kiefer et al.[1] (KKSST) reported schlieren shock tube measurements of vibrational relaxation, incubation, and unimolecular rate constants for the HF elimination from 1,1,1-trifluoroethane (TFE). One of the surprising results of this study was that the pressure dependence of the unimolecular rate constants is not accurately modeled using RRKM theory, which is based on concepts introduced by Rice, Ramsperger, Kassel, and Marcus.[2−4] Instead of continuing to increase with pressure as predicted by RRKM theory, the experimental rate constants at the three highest pressures are essentially equal, as shown in Figure 3 in KKSST and in Figure 1 in the recent publication on this reaction from our group.[5]

KKSST[1] and Kiefer (private communication) suggest that their data can be explained by a non-RRKM model in which the torsional vibrational mode is preferentially excited by collisions following the shock. They argue that this mode sequesters vibrational energy, which flows only very slowly to the reaction coordinate. Thus, when TFE has energy greater than the reaction critical energy, it reacts at a rate controlled by slow (~10^8 s^{-1}) intramolecular vibrational energy redistribution (IVR) between the sequestered modes and the remaining vibrational degrees of freedom. These and other arguments made by KKSST and Kiefer are summarized in ref 5.

In ref 5, master equation simulations of the KKSST experiments and the chemical activation experiments of Marcoux and Setser[6] were reported. Several master equation models were explored, including one in which IVR is explicitly included according to the local random matrix theory (LRMT) of Leitner and Wolynes.[7] The LRMT is used to locate the energy threshold at which IVR is predicted to become very rapid, and to calculate IVR time constants at higher energies. The LRMT predictions previously made for other systems are generally in good agreement with experimental results.[8−10] For TFE the LRMT predicts that the IVR threshold is about 10 kcal mol^{-1} above the zero point energy and that IVR is extremely rapid at the reaction threshold itself, which is nearly 60 kcal mol^{-1} higher in energy.[1,5] Since the IVR rates are predicted to be so fast, they are not rate-limiting and their over-all effect is negligible. Using the LRMT in the master equation simulations does not fit the KKSST data set. However, an empirical non-RRKM model was found that gives results similar to the KKSST experimental data. This model consists of simply truncating $k(E)$ at 1.5×10^7 s^{-1}. This model has no theoretical justification; it simply fits the KKSST data set.

Master equation simulations in paper I also showed that the chemical activation data of Marcoux and Setser[6] do not constrain the model, because free adjustment of the (unknown) energy transfer parameters allow all of the models to produce good fits to the chemical activation data. It was concluded in ref 5 that the available experimental data do not allow one to reach a definite conclusion about whether slow IVR is a reasonable explanation of the unusual pressure dependence measured by KKSST.

In the present paper, we employ classical trajectory methods to test the proposal by KKSST and Kiefer that energy is sequestered in the torsional mode. When the torsion in TFE

† Part of the special issue "David M. Golden Festschrift".

* Corresponding author. E-mail: jrbarker@umich.edu.

‡ Department of Atmospheric, Oceanic, and Space Sciences, University of Michigan.

§ Department of Chemistry, University of Michigan.

10.1021/jp0568024 CCC: $33.50
Published on Web 02/15/2006

contains energy below the torsional barrier, the harmonic oscillator approximation is reasonably accurate, but the large amplitude hindered rotation that takes place at higher energies is extremely anharmonic. Thus, we turn to classical trajectories, which allow for simulation with an anharmonic potential energy surface of full dimensionality. At low energies, classical mechanics cannot reproduce quantum effects like conservation of zero point energy and interference,[11] but these effects are of less importance at energies as high as the reaction threshold for HF elimination in TFE. In TFE, the reaction critical energy (defined as the zero point energy difference between transition state and reactant) is about 70 kcal mol^{-1}. Since the zero point energies of TFE and the transition state are about 36 and 31 kcal mol^{-1}, respectively,[1] the classical reaction threshold is about 75 kcal mol^{-1} above the bottom of the potential energy well.

HF elimination from TFE has been studied previously using classical trajectory methods.[12,13] Benito and Santamaría[12,13] used the transition state structure as a starting point and then used classical trajectories to investigate the product energy distributions. With several different empirical potential energy surfaces, these authors found that the distribution of vibrational energy in the HF product was nonstatistical. The authors did not investigate IVR within TFE, however, which is the focus of the present work.

Classical trajectory methods are useful for studying IVR since these methods integrate the classical equations of motion, thus allowing the time evolution of a system to be simulated. Despite uncertainties in the accuracy of the potential energy surfaces, these methods have helped further understanding of IVR and energy transfer. Consider, for example, a series of studies in which classical trajectory methods were used to study a system quite similar to the one considered here: the unimolecular dissociation of 1,2-difluoroethane (DFE).[14−18] These studies established that C−C bond fission and C−H bond fission in DFE are nonstatistical, but HF elimination from DFE is statistical. On the basis of the calculations, three conditions were identified[14,18] as determining whether a reaction is nonstatistical: (1) the internal energy is close to the dissociation threshold, (2) motion along the reaction coordinate does not produce large energetic changes in one or more bonds in the remainder of the molecule, and (3) there exists a formation coordinate for the activated reactant that is strongly coupled to the dissociation coordinate but only weakly coupled to the other internal coordinates of the molecule. Later work on DFE relied on using power spectra to demonstrate the validity of these guidelines.[14] This later study also established qualitative guidelines for using power spectra to judge the statistical/nonstatistical nature of chemical reactions. We highlight the work on DFE because it provides a template for studying the statistical nature of chemical reactions, and also because of the similarity of DFE to TFE.

In this work we use two empirical potential energy functions and the molecular dynamics program VENUS96[19] (VENUS) to investigate IVR within TFE. The two potential energy functions are parametrized to reproduce the equilibrium geometry and normal-mode frequencies for TFE. These empirical potential energy functions do not include the HF elimination reaction channel. Our objective is simply to study IVR involving the torsional mode and to discuss the non-RRKM model proposed by KKSST and Kiefer in light of our findings.

The principal result of this study is that for energies near the reaction threshold, the time constants for energy to leave the torsion are at least 1000 times shorter than the 10 ns estimate of KKSST.[1] Although our results cannot prove that the non-RRKM effects described by KKSST and Kiefer are unimportant in the TFE reaction, they strongly suggest that IVR involving the torsion is not rate-limiting at energies near the reaction threshold.

II. Theoretical Methods

The VENUS program has been described in detail elsewhere.[19] Briefly, the program integrates Hamilton's equations of motion based on a user-supplied potential energy function. The potential energy is first formulated in curvilinear internal coordinates and then transformed to Cartesian coordinates.[20] This procedure ensures that the accuracy of the Hamiltonian depends only on the potential energy, since no terms are neglected in the kinetic energy expression.[20]

Potential Energy Functions. The multidimensional potential energy surface for TFE is expressed in VENUS by using a potential energy function (PEF). The two potential energy functions used to describe TFE in the present work are based on the following equation:

$$
\begin{aligned}
V = &\sum_{i=1}^{1} D_{CC}[1 - \exp^{-\beta_{CC}(r_{CC} - r_{CC}^{0})}]^2 + \\
&\sum_{i=1}^{3} D_{CF}[1 - \exp^{-\beta_{CC}(r_{CF}^{i} - r_{CF}^{0})}]^2 + \\
&\sum_{i=1}^{3} D_{CH}[1 - \exp^{-\beta_{CH}(r_{CH}^{i} - r_{CH}^{0})}]^2 + \\
&\sum_{i=1}^{3} \frac{1}{2} f_{CCH} S(r_{CC}) S(r_{CH}^{i})(\theta_{CCH}^{i} - \theta_{CCH}^{0})^2 + \\
&\sum_{i=1}^{3} \frac{1}{2} f_{CCF} S(r_{CC}) S(r_{CF}^{i})(\theta_{CCF}^{i} - \theta_{CCF}^{0})^2 + \\
&\sum_{i<j}^{3} \frac{1}{2} f_{HCH} S(r_{CH}^{i}) S(r_{CH}^{j})(\theta_{HCH}^{i} - \theta_{HCH}^{0})^2 + \\
&\sum_{i<j}^{3} \frac{1}{2} f_{FCF} S(r_{CF}^{i}) S(r_{CF}^{j})(\theta_{FCF}^{i} - \theta_{FCF}^{0})^2 + \\
&\sum_{i=1}^{9} \sum_{n=1}^{3} \frac{k_d^{n}}{2} S(r_i)[1 + \cos(n\tau_i - \gamma_n)] + \\
&\sum_{i=1}^{3} f_{(CF-CC)}(r_{CF}^{i} - r_{CF}^{0})(r_{CC} - r_{CC}^{0}) + \\
&\sum_{i=1}^{3} \sum_{j=1}^{3} g_{(CF-FCF)}(r_{CF}^{i} - r_{CF}^{0})(\theta_{FCF}^{j} - \theta_{FCF}^{0}) + \\
&\sum_{i=1}^{3} \sum_{j=1}^{3} h_{(CCF-FCF)}(\theta_{CCF}^{i} - \theta_{CCF}^{0})(\theta_{FCF}^{j} - \theta_{FCF}^{0}) \quad (1)
\end{aligned}
$$

In eq 1 the first three terms indicate that bond stretches are modeled using Morse oscillators, the next four terms indicate that bond bending is modeled using the harmonic approximation, the eighth term accounts for the potential energy associated with the dihedral angles, and the last three terms describe nondiagonal sretch−stretch, stretch−bend, and bend−bend interactions, respectively. Two lettered subscripts denote bonds, and three letter subscripts denote bond angles. For bond angles, the middle index denotes the central atom of the angle. In eq 1 the D_{ij} terms are the bond dissociation energies; β_{ij} are the Morse exponential terms; r_{ij} are the bond lengths; θ_{ijk} are the bond angles; k_d^n is the contribution of the potential barrier to internal rotation that depends on dihedral angle τ_i with periodicity n; γ_n

TABLE 1: Potential Energy Function Parameters

parameter	value
D_{CC}[a]	101.33 kcal mol^{-1}
D_{CH}[a]	106.69 kcal mol^{-1}
D_{CF}[a]	124.80 kcal mol^{-1}
β_{CC}	1.8149 Å^{-1}
β_{CH}	1.8911 Å^{-1}
β_{CF}	1.8789 Å^{-1}
f_{CCH}	0.6426 mdyn Å/rad^2
f_{CCF}	2.1058 mdyn Å/rad^2
f_{HCH}	0.3468 mdyn Å/rad^2
f_{FCF}	0.7837 mdyn Å/rad^2
$f_{(CF-CC)}{}^0$	1.1610 mdyn/Å
$g_{(CF-FCF)}{}^0$	0.3447 mdyn/rad
$h_{(CCF-FCF)}{}^0$	−0.4057 mdyn Å/rad^2
$k_d{}^1$	0.0 kcal mol^{-1}
$k_d{}^2$	0.0 kcal mol^{-1}
$k_d{}^3$ (Note b)	0.3611 kcal mol^{-1}
γ_n (Note c)	0.0 degrees
$r_{CC}{}^0$	1.5018 Å
$r_{CH}{}^0$	1.0875 Å
$r_{CF}{}^0$	1.3499 Å
$\theta_{CCH}{}^0$	109.334°
$\theta_{CCF}{}^0$	111.809°
$\theta_{HCH}{}^0$	109.608°
$\theta_{CFC}{}^0$	107.035°
all C	1.0 Å^{-1}

[a] Values from ref 36. [b] $k_d{}^3$ is the barrier to internal rotation (3.25 kcal mol^{-1}) divided by nine (the number of dihedral angles.) [c] For all n.

are the phase angles that also depend on the periodicity. The superscript 0 in eq 1 refers to the value of the term at the minimum energy equilibrium geometry. The nondiagonal force constants in eq 1 are defined as

$$f_{(CF-CC)} = f_{(CF-CC)}{}^0 S(r_{CF}{}^i) S(r_{CC}) \quad (2)$$

$$g_{(CF-FCF)} = g_{(CF-FCF)}{}^0 S(r_{CF}{}^i) S(r_{CF}{}^j) S(r_{CF}{}^k) \quad (3)$$

$$h_{(CCF-FCF)} = h_{(CCF-FCF)}{}^0 S(r_{CC}) S(r_{CF}{}^i) S(r_{CF}{}^j) S(r_{CF}{}^k) \quad (4)$$

where the switching functions in all cases are defined as

$$S(r_i) = \exp[-C(r_i - r_i{}^0)] \quad (5)$$

In eq 5, C is the attenuation constant and serves to attenuate the potential energy of an interaction based on the distance two bonded atoms are from their equilibrium distance.

In this study, the "full" PEF used all terms in eq 1 and the "simple" PEF neglected the three nondiagonal interactions in eq 1. The adjustable parameters in eq 1 were determined using the Levenberg−Marquardt nonlinear least squares algorithm[21] to minimize differences between the vibrational frequencies calculated with the full PEF and those calculated[22] using quantum chemical methods (the B3LYP/cc-pVTZ level of theory). The simple PEF was not reparametrized but used the same optimized parameters as the full PEF. See Table 1 for a complete list of the parameters for the full PEF. In Table 2, we compare the experimental vibrational frequencies[23] to those calculated[22] at the B3LYP/cc-pVTZ level of theory and those computed using the two PEFs. For both PEFs the bond lengths agree with those calculated at the B3LYP/cc-pVTZ level of theory to within ±0.001 Å and the bond angles agree to within ±0.002°. The vibrational frequencies obtained using the full PEF are in excellent agreement with the quantum chemical calculations, whereas those obtained using the simple PEF are still in very good agreement.

TABLE 2: Vibrational Frequencies

experimental [23,a]	B3LYP/ cc-pVTZ[22,b]	full PEF[b]	simple PEF[b]
220 (A_2)[c] torsion	226	237	237
364 (E) CF_3 rocking	362	361	361
541 (E) CF_3 asym def	537	533	533
603 (A_1) CF_3 sym def	597	592	517
831 (A_1) CC str	829	815	722
969 (E) CH_3 rocking	969	963	963
1224 (E) CF_3 asym str	1224	1222	1222
1281 (A_1) CF_3 sym str	1280	1265	1264
1407 (A_1) CH_3 sym def.	1431	1447	1506
1457 (E) CH_3 asym def.	1485	1497	1496
2975 (A_1) CH_3 sym str	3067	3034	3034
3034 (E) CH_3 asym str	3148	3159	3159

[a] Fundamental vibrational frequencies (cm^{-1}). [b] Harmonic vibrational frequencies (cm^{-1}). [c] Symmetry species in the C_{3v} point group.

We use two PEFs in this work because the nondiagonal interactions in the full PEF result in C−H bond fission at an unrealistically low energy (60 kcal mol^{-1}). This energy is lower than needed for our investigation of IVR. Therefore, we use the simple PEF, which omits the explicit nondiagonal interactions introduced in the last three terms of eq 1, to investigate energies greater than the reaction threshold. Later we will show the results obtained with the two PEFs are similar for energies below the reaction threshold. On the basis of this result we expect the simple PEF will provide a reasonable description of the interactions in TFE at energies greater than the reaction threshold.

Initial Vibrational Energy Distributions. The microcanonical initialization procedure in VENUS assumes that all vibrational degrees of freedom are separable harmonic oscillators.[19] With this assumption, normal coordinate displacement vectors and velocities are randomly selected for all the normal modes such that the total energy in the normal modes matches a user-supplied vibrational energy. If the energy computed with the initial guesses for the normal coordinate displacements and velocities does not match the desired vibrational energy to within one tenth of a percent, the normal coordinate displacement vectors and velocities are scaled until this convergence criterion is met.[19] We refer to this energy initialization procedure as the standard initialization scheme.

We modified the standard initialization scheme so that the torsional normal coordinate could be initialized with a large amount of energy relative to the other normal modes. This was accomplished by specifying that only a fraction Z of the normal coordinate displacements and velocities of each other normal coordinate were used to compute the energy for these vibrational degrees of freedom. The other normal coordinate displacements and velocities were then fixed at their initial values and not scaled to match the specified total vibrational energy; only the normal coordinate displacements and velocities for the torsional normal coordinate were scaled to match the total vibrational energy. We refer to this energy initialization procedure as the loaded initialization scheme. In all cases, Z was set to 0.375. It should be noted that the loaded initialization scheme is quite inefficient. Instead of generating trajectories with a specific energy, trajectories were initialized with a large range of energies. This fact posed no problem though since trajectories that were initialized with the desired amount of energy were simply extracted from the data set containing information for all trajectories. More details on the efficiency of this energy initialization scheme will be given in the next section.

Torsional Energy Analysis. While VENUS can calculate the vibrational energy in each normal mode, the procedure it

uses is not valid for a molecule rotating in space. This is because the instantaneous energies in the normal modes are obtained from instantaneous atomic displacements from a space-fixed reference geometry. If during the simulation the instantaneous geometry rotates away from the space-fixed reference geometry, the atomic displacements and consequently the normal mode energies will not be correct. If instead the space-fixed reference geometry was transformed to the Eckart rotating frame, normal mode energies could be calculated for the case of a rotating molecule, but this feature is not available in VENUS96 (and is cumbersome to implement).

In their study of collisional energy transfer involving the torsion in ethane, Linhananta and Lim calculated the angular momentum for each methyl rotor separately and then subtracted the two angular momenta to obtain the energy in the torsion.[24] We have adopted a method that is in principle equivalent, but explicitly uses the FCCH dihedral angles. It is important to note that, for finite internal energy, the "normal" modes are not separable, and therefore, both methods of determining the "torsion" internal energy are affected by other modes.

The torsional energy is calculated using

$$E_k = \frac{1}{2} I_R \omega^2 \tag{6}$$

where E_k is the kinetic energy of the rotor, I_R is the reduced moment of inertia of TFE, and ω is the angular velocity. The reduced moment of inertia is given by

$$I_R = \frac{I_{CH_3} I_{CF_3}}{I_{CH_3} + I_{CF_3}} \tag{7}$$

where I_{CH_3} and I_{CF_3} are respectively, the moments of inertia of the CH_3 and CF_3 groups. The moments of inertia for the groups are calculated using

$$I = \sum_{i=1}^{3} m_i r_i^2 \tag{8}$$

where m_i and r_i are respectively, the masses of the hydrogen or fluorine, and the distance each hydrogen or fluorine atom is from the symmetry axis (the C−C bond). The angular velocity, ω is calculated using

$$\omega = \frac{d\tau}{dt} \approx \frac{\Delta\tau}{\Delta t} \tag{9}$$

where τ is the dihedral angle and t is time. In the simulations $\Delta\tau$ is the difference in the dihedral angle between two consecutive integration cycles. $\Delta\tau$ is calculated by summing the signed changes in each of the nine FCCH dihedral angles and dividing this quantity by nine to obtain an average change in dihedral angle. The average angular velocity is then calculated by dividing by the time between integration cycles (0.0007 ps), and this quantity is then used in eq 6. The total energy in the rotor is calculated by averaging the potential and kinetic energies from consecutive integration cycles and adding the resulting averaged values.

Since the interpretation of our results depends on the accuracy of the methodology used to calculate the torsional energy, we use two limiting cases to test the method. In one case, we used the loaded initialization scheme to place the total energy in the torsion. In the other case, we used a variant of the loaded initialization scheme and distributed the energy microcanonically in all vibrational degrees of freedom except the torsion. At the beginning of a trajectory initialized with the vibrational energy placed in the torsion, the torsional energy calculated using our scheme matches the total molecular energy VENUS calculates to within 0.2% for energies from 5 to 120 kcal mol^{-1}. When no vibrational energy is placed in the torsional normal mode but energies from 5 to 120 kcal mol^{-1} are placed in the other modes, our scheme calculates a torsional energy of less than 0.3% of the total molecular energy (note that there should be no energy in the torsion for this case). The energy in the torsion is nonzero because the normal modes are not separable. The superposition of the normal coordinate displacement vectors and velocities from the other normal modes contributes to the angular velocity and, hence, to the calculated torsion energy.

Power Spectral Analysis. Power spectra have been used extensively to study IVR within molecules.[14,18,25−28] We compute the power spectrum using

$$I(\nu) = \frac{1}{T}\int_0^T |\langle q(t)\rangle \cos(2\pi\nu t)\, dt|^2 \tag{10}$$

where t is time, ν is the frequency at which the power spectrum is to be evaluated, T is the total time duration of a simulation, and $q(t)$ denotes one of the internal coordinates of TFE. As noted previously by other researchers,[14] using $q(t)$ in the cosine transform results in a power spectrum that emphasizes the onset of transitions between prominent spectral features.

In this work the angular velocities of the nine FCCH dihedral angles are $q(t)$. Using a protocol similar to that used by Chang et al.,[14] we calculate the power spectrum for a set of reduced internal coordinates $q_r(t)$ defined as

$$q_r(t) = \frac{q(t)}{|q_{max}|} \tag{11}$$

where q_{max} is the maximum value of the internal coordinate that is observed during a trajectory. The $q_r(t)$ are therefore dimensionless and have values between +1 and −1. For a single trajectory, all nine $q_r(t)$ are calculated and used to generate nine power spectra. The power spectra are then added to give a composite power spectrum. We always report the composite power spectrum. Each power spectrum was obtained by evaluating eq 10 numerically using a frequency step size of 1.0 cm^{-1}.

III. Results and Discussion

Unless stated otherwise all results that follow are ensemble averages for at least 500 trajectories. All trajectories used an integration step size of 0.1 fs. Energy conservation for the longest trajectories considered here (1 ns) was tested by averaging the difference between the initial and final total energies for 10 trajectories of 1 ns duration. The average differences were about 0.385 kcal mol^{-1} for trajectories at 100 kcal mol^{-1} total vibrational energy and 0.00483 kcal mol^{-1} for trajectories with 30 kcal mol^{-1} of total vibrational energy. The rotational temperature in all simulations was 0.1 K; calculations (not reported here) with 100 kcal mol^{-1} total vibrational energy and rotational temperatures of 0.1, 300, and 2000 K (where the total energy increased from 100 to 106 kcal mol^{-1}) gave power spectra and torsional energy distributions that are the same, within the statistical uncertainties.

Standard Initialization Results. One method for probing the torsional energy distribution is to monitor the ensemble averaged torsional energy. In Figure 1, we show the ensemble averaged torsional energies for various total vibrational energies. Panels a−c depict the torsional energy distributions obtained

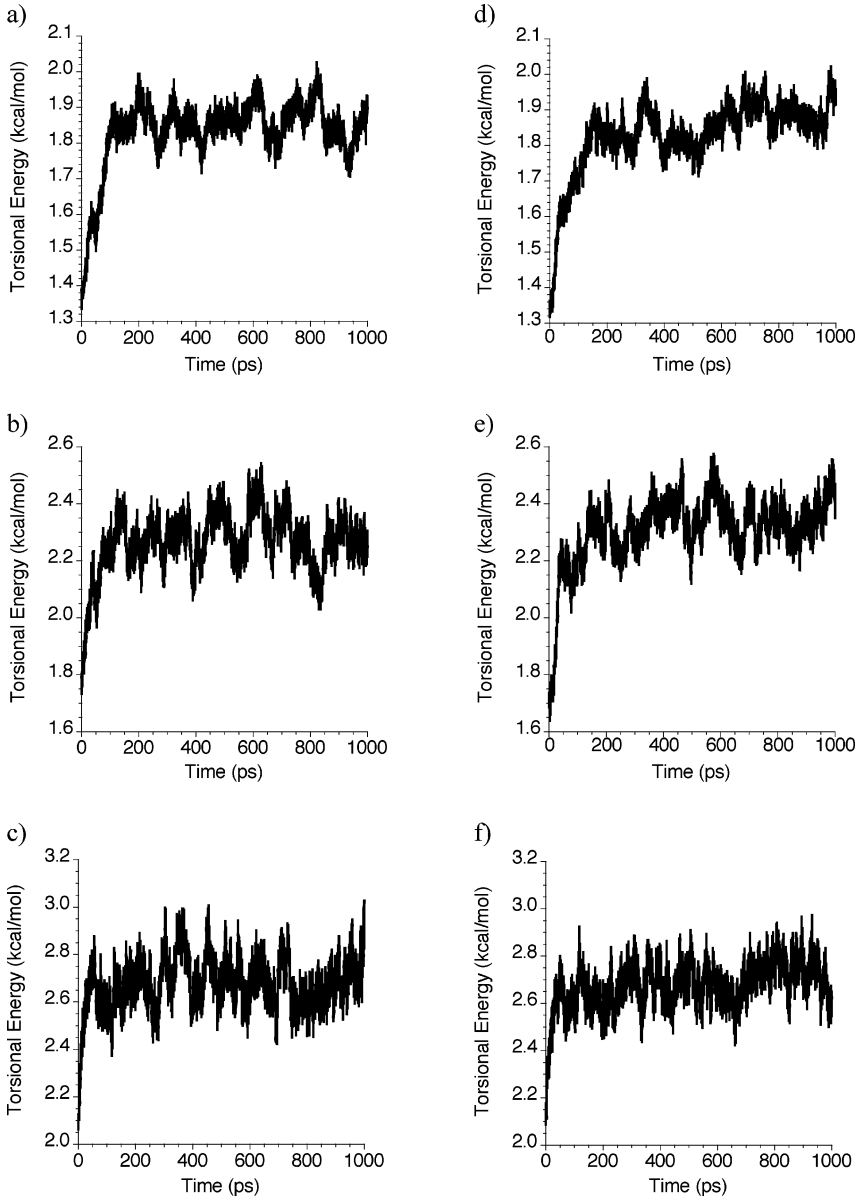

Figure 1. Ensemble averaged torsional energies from trajectories initialized using the standard initialization scheme. Panels a−c were obtained with the full PEF and panels d−f were obtained using the simple PEF. The data in panels a−c are for 30, 40, and 50 kcal mol^{-1} of total vibrational energy, respectively. Data in panels d−f are for the same energies as panels a−c.

TABLE 3: Average Torsional and Equipartition Energies[a]

total vibrational energy [a]	full PEF $E_{torsion}$	simple PEF $E_{torsion}$	equipartition energy
30	1.83	1.83	1.67
40	2.27	2.31	2.22
50	2.68	2.67	2.78

[a] kcal mol^{-1}

using the full PEF, and panels d−f show data obtained using the simple PEF. In all cases, the average torsional energy increases rapidly and then fluctuates about an energy that is close to that predicted by the equipartition of energy. The average torsional energies and the equipartition energies are shown in Table 3. We note that the equipartition values do not strictly apply to the torsional mode, since the potential energy of the torsional mode is not a quadratic function of the coordinates.[29] We give the equipartition values only to indicate that the energy in the torsional mode is not drastically different from the energy predicted for TFE if it were modeled as a collection of harmonic oscillators. It is noteworthy that the microcanonical energy-momentum selection scheme in VENUS, which is based on harmonic oscillators, is reasonably successful, but not perfect, in selecting initial conditions for this highly anharmonic mode.

It is important to observe that the average torsional energies obtained using the two PEFs are nearly identical. This result indicates that the nondiagonal contributions do not have much of an impact on the average torsional energy, at least at the total vibrational energies considered here. The important conclusion to draw from the data in Figure 1a−f is that the time dependence of the ensemble averaged torsional energies does not indicate that anomalous amounts of energy are being sequestered in the torsional mode for long periods of time.

While the ensemble averaged results are useful for depicting how the system behaves on average, it is also instructive to monitor the torsional energy for individual trajectories. In Figure 2, we show the torsional energies from single trajectories initialized using the standard initialization scheme with total vibrational energies of 30 and 100 kcal mol^{-1}, respectively. The results in Figure 2 show that a significant fraction of the total

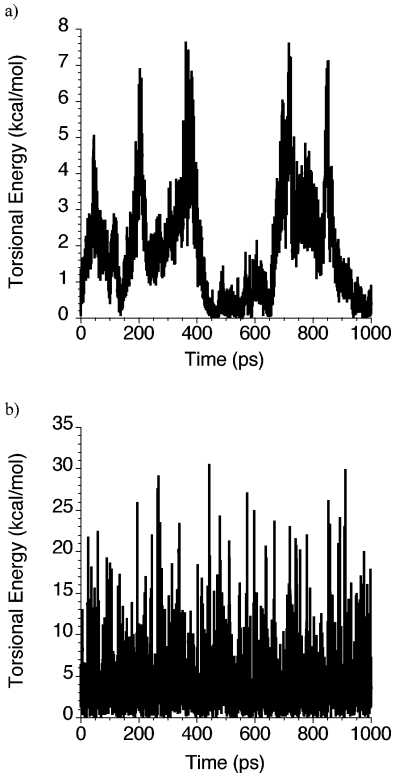

Figure 2. Torsional energies from a single trajectory initialized using the standard initialization scheme: (a) 30 kcal mol^{-1} of total vibrational energy; (b) 100 kcal mol^{-1} of total vibrational energy. These data were obtained using the simple PEF.

available vibrational energy rapidly flows in to and out of the torsion. If energy were isolated in the torsion, one would expect much smaller energy fluctuations than are observed in Figure 2.

Loaded Initialization Results. To test the conceptual model proposed by KKSST and Kiefer requires putting a substantial amount of energy in the torsional mode and monitoring the time it takes for the energy to redistribute to the remaining vibrational degrees of freedom. This was accomplished by using the loaded initialization scheme. Since using the full PEF sometimes resulted in trajectories that dissociated at relatively low energies, as noted earlier, we determined time constants for energy relaxation from the torsional mode using the simple PEF. In Figure 3 we show the ensemble averaged torsional energies for simulations in which 25% ± 10% and 45% ± 10% of the total vibrational energy (80, 100, and 120 kcal mol^{-1}) is placed in the torsional normal mode. As noted earlier the loaded energy initialization scheme is inefficient. Out of a total of 2000 trajectories with fraction $Z = 0.375$, only about 525 were initialized with 25% ± 10% and about 325 of the 2000 were initialized with 45% ± 10%. Therefore, the results in Figure 3a are the ensemble averaged results obtained using about 525 trajectories, and the results in Figure 3b are the ensemble averaged results obtained using about 325 trajectories.

The decay of the ensemble averaged torsional energies in Figure 3 is well described by a single-exponential function:

$$E(t) = c_1 \exp(-t/\tau_{tor}) + c_3 \qquad (12)$$

where $E(t)$ in eq 12 is the energy in the torsional mode which depends on the time (t), c_1 and c_3 are fitted parameters, and τ_{tor} is a time constant describing energy flow out of the torsional mode, i.e., an IVR time constant. In general IVR exhibits multiple time scales and the time scales themselves depend on

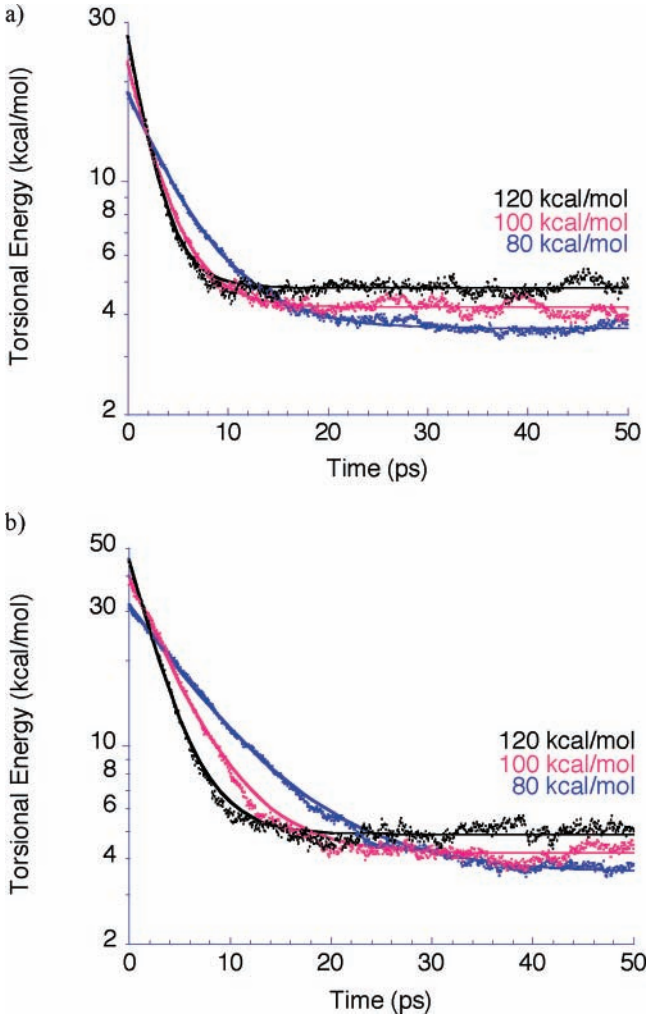

Figure 3. Average torsional energies for trajectories initialized using the loaded initialization scheme. (a) 25% ± 10% of the total energy in the torsion; (b) 45% ± 10% of the total energy in the torsion. Shown in both panels are data for total vibrational energies of 80, 100, and 120 kcal mol^{-1}. The data in both panels were obtained using the simple PEF. The solid lines are fits to the data using a nonlinear least squares routine.

TABLE 4: IVR Time Constants

	time constants (ps)	
E_{vib} (total vibrational energy, kcal mol^{-1})	$E_{torsion}/E_{vib}$ = 0.25 ± 0.10	$E_{torsion}/E_{vib}$ = 0.45 ± 0.10
80	5.2	8.0
100	3.0	4.8
120	2.1	3.0

the way in which the molecule is excited. Here we are only concerned with energy flow out of the torsional mode and consequently in what follows reference to the IVR time constant always refers to τ_{tor}. See Table 4 for the IVR time constants extracted from the data in Figure 3.

As expected, the IVR time constants in Table 4 show a clear dependence on the amount of energy initially residing in the torsional mode. The greater the energy that is initially placed in the torsional mode the longer the IVR time constant. In all cases the IVR time constants are less than 10 ps, which is 3 orders of magnitude faster than the time constant estimated by KKSST.[1] In the limit that all of the vibrational energy is placed in the torsional mode, very long times (at least several nanoseconds) will be needed for the energy to redistribute. It is also noteworthy that for each case considered in Figure 3 only

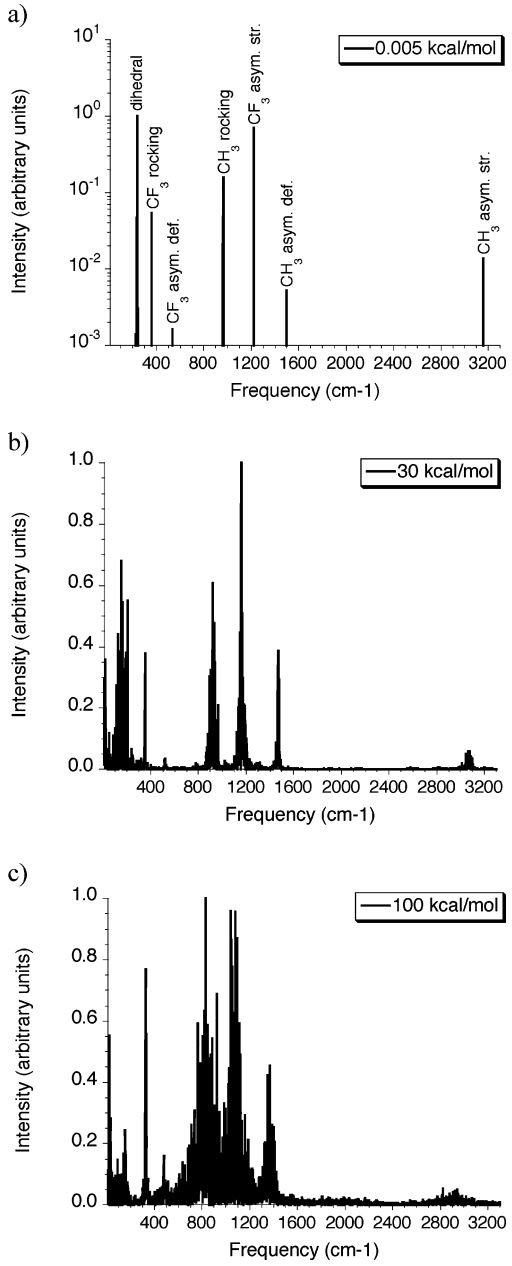

Figure 4. Power spectra at various total vibrational energies for trajectories initialized using the standard initialization scheme. The data in all panels was obtained using the simple PEF.

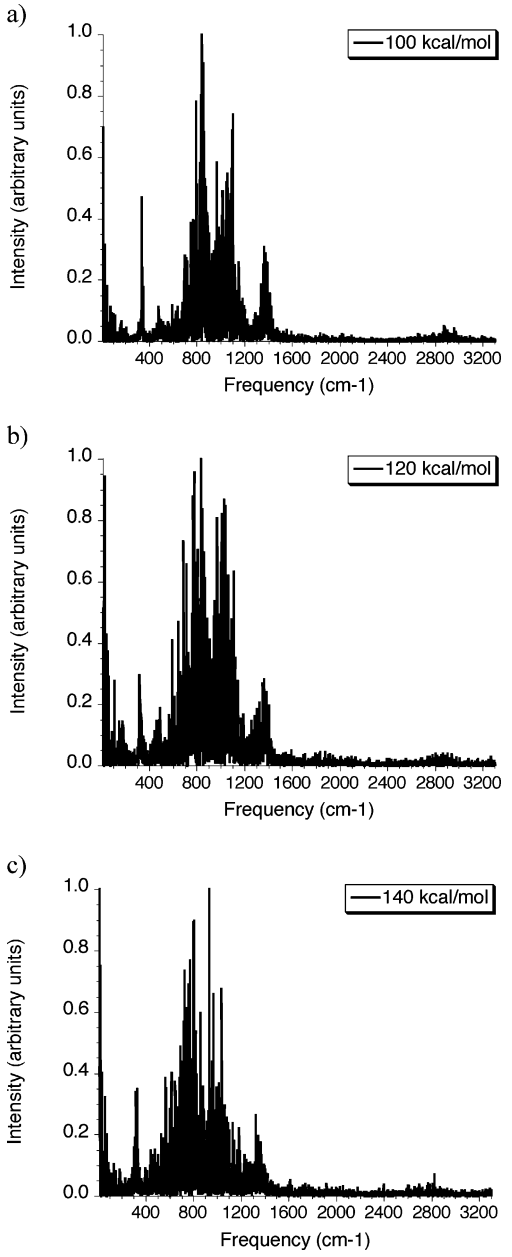

Figure 5. Power spectra at various total vibrational energies for trajectories initialized using the loaded initialization scheme. These data are for a single trajectory in which 28% of the total vibrational energy was initially placed in the torsional mode. The data in all panels was obtained using the simple PEF.

50 ps are needed for the average torsional energy to become equal to the ensemble averaged torsional energy obtained for 500 trajectories of 1 ns duration. This result indicates that there is not a slow component to the relaxation.

The trend observed in Figure 3 seems to contradict the results in Figure 1, where the time constant becomes shorter as the total vibrational energy is increased. However, both can be understood if the rate of IVR is controlled largely by the amount of energy in the *other* modes. As the other modes become more excited, the asymmetric methyl deformations become more extreme, resulting in breaking the high symmetry of the equilibrium structure. This creates more resistance to internal rotation and provides a coupling mechanism that enhances the IVR rate. This is an argument first presented in ref 5.

Power Spectra Results. All power spectra were obtained for single trajectories of 50 ps duration. Power spectra for multiple trajectories were investigated, and it was found that all of the spectra are qualitatively similar. The intensities of all peaks are normalized relative to the most intense peak at a frequency greater than 10 cm^{-1}. This choice was made because there was often a large intensity at very low frequency.

In Figure 4, we show power spectra at vibrational energies of 0.005, 30 (approximately the zero point energy (ZPE)), and 100 kcal mol^{-1} (approximately the ZPE plus the reaction threshold energy), for trajectories initialized using the standard initialization procedure. As expected,[27] Figure 4a shows that, at low energy, the spectral transitions are sharp and match the normal-mode frequencies exactly.

In general, as the total vibrational energy is increased the spectral features broaden and undergo red-shifting. With the exception of the CF_3 rocking and the torsion modes, the transitions in panel c are red shifted by about 100 cm^{-1} in comparison to the normal-mode frequencies. The red-shifting

and broadening are the result of intermode coupling. The intermode coulpling occurs via the kinetic energy couplings in the Hamiltonian. A striking feature of these spectra is that the torsional mode is not isolated from the other vibrational modes. This is evident in Figure 4, parts b and c, where the transition at the torsional frequency of 237 cm^{-1} broadens and appears to become less intense. The high-frequency CH stretch transitions near 3000 cm^{-1} also broaden and undergo red-shifting as the total vibrational energy increases, apparently due to coupling with other modes. Note that red-shifting results in better frequency matching with the overtones of some of the mid-frequency transitions. This can result in enhanced IVR rates.[30]

In Figure 5, are shown power spectra for trajectories initialized using the loaded initialization scheme. These power spectra were obtained at total vibrational energies of 100, 120, and 140 kcal mol^{-1} with approximately 28% of the total vibrational energy initially in the torsional mode. As the total vibrational energy increases, broadening of all transitions is very clear. Again, the torsional mode transition is smeared out and indistinct, indicating that the torsional mode is coupled to other modes. As was the case in Figure 4, with the exception of the CF_3 rocking transition and the torsion, the transitions in all spectra are red-shifted from the normal-mode frequencies by about 100 cm^{-1}. In the spectral window between 350 and 1500 cm^{-1}, which contains nine of the 12 harmonic frequencies, we see a significant broadening as the vibrational energy is increased. At 140 kcal mol^{-1} of vibrational energy the spectral identity of specific transitions has become difficult to assign. There is also an increase in the number and intensity of transitions between about 1600 and 2800 cm^{-1}as the vibrational energy is increased. Overall the spectra show that the vibrational modes are strongly coupled and that the coupling increases as the total vibrational energy increases. Although these spectra do not exhibit the "grassiness" that has been attributed to statistical systems, none of the transitions is completely isolated.[14] This result suggests that TFE should be well described by statistical theories like RRKM theory.

IV. Conclusions and Implications for the KKSST non-RRKM Model

Using two empirical PEFs and classical trajectory calculations we have studied IVR in TFE. In contrast to KKSST[1] and Kiefer's non-RRKM model, which assumes that IVR takes place on a time scale of ~10 ns, we find that the time constant for energy to leave the torsion proceeds about 1000 times as fast—typically <10 ps at energies greater than the classical reaction threshold energy. Furthermore, the rate of decay depends largely on the amount of energy in the other vibrational energy modes. This is explained if the methyl deformations interfere with the internal rotation and thus provide a mechanism for enhanced IVR.[5] Power spectra obtained for a range of energies provide evidence that coupling between the vibrational modes is substantial and increases as the total vibrational energy in the molecule increases. In all cases we find that IVR involving the torsion is fast and that the torsion is not isolated from the other vibrational modes.

One must exercise some caution, when interpreting these results. The accuracy of the results depends primarily on how accurately the PEF describes the "real" TFE molecule. We have chosen to use simple, conventional PEFs that are parametrized to reproduce only the equilibrium geometry and vibrational frequencies of TFE. There is no guarantee that these PEFs are accurate for geometries far from equilibrium. Additionally, previous researchers have shown that IVR can be very sensitive to details of the PEF.[20] However, the simple PEF minimizes off-diagonal interactions and therefore probably has less internal coupling than the true PEF. If this is the case, then the calculated IVR time constants are probably upper limits to the correct values.

It is informative to review and discuss the model proposed by KKSST[1] and Kiefer[37] to explain the unusual pressure dependence of the TFE data. Their model is summarized in ref 5. They envision rapid collisional energy transfer mostly to the torsional mode, which remains only weakly coupled to the other modes at high energies due to its high symmetry. Furthermore, when the torsion is excited, the distortion of the CH_3 and CF_3 rotors needed to achieve the geometry of the transition state introduces >20 kcal mol^{-1} increase in the energy requirement for reaction. This conclusion is based on a calculation carried out by L. Harding in which the two distorted rotors were "frozen" in the transition state geometry and then forced to rotate around the C−C axis.[38] This added energy effectively raises the critical energy for reaction when the torsion is excited, resulting in the non-RRKM effect. Thus, according to this proposed model, excitation of the isolated torsion both sequesters energy, making it unavailable for reaction, and increases the reaction critical energy, further slowing the reaction.

The validity of KKSST and Kiefer's non-RRKM model rests on the assumptions that energy is selectively transferred to the torsion and then becomes isolated in the torsional mode. Below the torsion barrier, the torsional states are nearly equally spaced and collisional activation from one torsion quantum state to the next will proceed with roughly the same rate constant, scaled by the vibrational quantum number, like a harmonic oscillator.[31] Above the barrier, however, the torsional states become more like free internal rotations where the energy difference between states become larger as the total energy is increased. At a torsional energy of ~20 kcal mol^{-1} above the zero level, for example, the hindered rotor states in TFE are about 400 cm^{-1} apart. As the energy differences between states increase, collisional excitation from one state to the next will become slower, due to the Boltzmann factor. Thus, there is an internal limitation in the rate of ladder climbing up the pure torsional states. In explaining ultrasound attenuation data, Lambert and Salter[32] showed that when the energy difference between states becomes large enough, further ladder climbing does not take place by pure torsional excitations, but via excitation of combinations of modes, where the energy differences between states are smaller.

Energy transfer in molecules that contain an internal rotor has also been studied computationally. For example, classical trajectory calculations on ethane[24] indicate that the torsion acts largely like a free rotor at moderate energies above the torsion barrier. Because it is coupled both to the over-all molecular rotations and to the molecular vibrations, the torsion acts as an efficient "gateway" to collisional energy transfer, which is mediated by rotations.[24] Thus, the torsion in ethane is not isolated, despite its high symmetry. Similar trajectory calculations on larger molecules have also shown that the torsion plays a significant role in collisional energy transfer.[33,34]

In addition to the experimental and computational energy transfer studies just cited, the local random matrix theory[7] (LRMT) of Leitner and Wolynes is designed to make predictions about IVR. LRMT is used to locate an IVR threshold, that is, it predicts an energy beyond which IVR will be fast. The LRMT has been applied to predict the IVR energy threshold and energy flow rates above the IVR threshold for dozens of modest-sized organic molecules, generally comparing well with experimental

results.[8−10] The LRMT IVR threshold and rates do not directly depend on the total density of states of the molecule, but on a local density of resonantly coupled states.[7,35] For TFE the LRMT predicts that the IVR threshold is about 10 kcal mol^{-1} above its zero point energy—an energy nearly 60 kcal mol^{-1} below the reaction threshold.[5]

In contrast with the LRMT, the present trajectory calculations do not show a distinct threshold for onset of IVR. To a large extent this may be due to the failure of classical mechanics to conserve zero point energy and its inability to capture the intrinsic quantum nature of IVR, as discussed in the context of the LRMT (which is a quantum mechanical model).[7,35] Thus, the present classical mechanical simulations cannot capture the details of IVR, although they can give semiquantitative insights. They agree with the LRMT in that IVR is expected to be rapid even at energies well below the reaction threshold. This is true even for the simple PEF, which minimizes coupling.

From these results, we conclude that even if collisional excitation of the torsional states is highly selective, the torsion is strongly coupled to the other vibrational modes and therefore energy randomization will be essentially complete before the next collision occurs. Thus, energy will not be selectively sequestered by the torsional mode, and another explanation must be found for the unusual pressure dependent data reported by KKSST.

Acknowledgment. Thanks go to John H. Kiefer, Lawrence Harding, Andrew H. Kim, Alexander Chimbayo, and Lawrence L. Lohr for discussions. P.J.S. wishes to thank John Boyd for helpful discussions on Fourier spectral methods. This work was funded in part by NASA (Upper Atmosphere Research Program), NASA (Planetary Atmospheres), and the NSF (Atmospheric Chemistry Division). Disclaimer: This material is based upon work supported in part by the National Science Foundation under Grant No. 0344102. Any opinions, findings, and conclusions or recommendations expressed in this material are those of the authors and do not necessarily reflect the views of the National Science Foundation.

References and Notes

(1) Kiefer, J. H.; Katapodis, C.; Santhanam, S.; Srinivasan, N. K.; Tranter, R. S. *J. Phys. Chem. A* **2004**, *108*, 2443−2450.
(2) Kassel, L. S. *J. Phys. Chem.* **1928**, *32*, 225.
(3) Marcus, R. A. *J. Chem. Phys.* **1952**, *20*, 359.
(4) Rice, O. K.; Ramsperger, H. C. *J. Am. Chem. Soc.* **1927**, *49*, 1617.
(5) Barker, J. R.; Stimac, P. J.; King, K. D.; Leitner, D. M. *J. Phys. Chem. A*, published on the Web December 15, 2005.
(6) Marcoux, P. J.; Setser, D. W. *J. Phys. Chem.* **1978**, *82*, 97−108.
(7) Leitner, D. M.; Wolynes, P. G. *J. Chem. Phys.* **1996**, *105*, 11226−11236.
(8) Bigwood, R.; Gruebele, M.; Leitner, D. M.; Wolynes, P. G. *Proc. Natl. Acad. Sci. U.S.A.* **1998**, *95*, 5960−5964.
(9) Gruebele, M.; Wolynes, P. G. *Acc. Chem. Res.* **2004**, *37*, 261−267.
(10) Leitner, D. M.; Wolynes, P. G. *Chem. Phys. Lett.* **1997**, *280*, 411−418.
(11) Sewell, T. D.; Thompson, D. L. *Int. J. Mod. Phys. B* **1996**, *11*, 1067.
(12) Benito, R. M.; Santamaria, J. *J. Phys. Chem.* **1988**, *92*, 5028−5035.
(13) Benito, R. M.; Santamaria, J. *Chem. Phys. Lett.* **1984**, *109*, 478−484.
(14) Chang, X. Y.; Sewell, T. D.; Raff, L. M.; Thompson, D. L. *J. Chem. Phys.* **1992**, *97*, 7354.
(15) Miller, J. A.; Klippenstein, S. J.; Raffy, C. *J. Phys. Chem. A* **2002**, *106*, 4904−4913.
(16) Raff, L. M. *J. Chem. Phys.* **1989**, *90*, 6313.
(17) Schranz, H. W.; Raff, L. M.; Thompson, D. L. *Chem. Phys. Lett.* **1991**, *182*, 455.
(18) Sewell, T. D.; Schranz, H. W.; Thompson, D. L.; Raff, L. M. *J. Chem. Phys.* **1991**, *95*, 8089.
(19) Hase, W. L.; Duchovic, R. J.; Hu, X.; Komornicki, A.; Lim, K. F.; Lu, D.-H.; Peslherbe, G. H.; Swamy, K. N.; Linde, S. R. V.; Varandas, A.; Wang, H.; Wolf, R. J. *Quantum Chem. Prog. Exchange Bull.* **1996**, *16*, 43.
(20) Lu, D. H.; Hase, W. L.; Wolf, R. J. *J. Chem. Phys.* **1986**, *85*, 4422.
(21) Press, W. H.; Teukolsky, S. A.; Vetterling, W. T.; Flannery, B. P. Levenberg−Marquardt Methodol. In *Numerical Recipes in FORTRAN The Art of Scientific Computing*, 2nd ed.; Cambridge University Press: New York, 1992; Vol. 1; pp 678−683.
(22) Johnson, R. D., III, Ed. *NIST Computational Chemistry Comparison and Benchmark Database, NIST Standard Reference Database Number 101 Release 12, August 2005*; NIST: Washington, DC, 2005. http://srdata.nist.gov/cccbdb.
(23) Nivellini, G.; Tullini, F.; Celli, A.; Becucci, M. *J. Chem. Soc., Faraday Trans.* **1998**, *94*, 2909.
(24) Linhananta, A.; Lim, K. F. *Phys. Chem. Chem. Phys.* **1999**, *1*, 3467−3471.
(25) Llorente, J. M. G.; Taylor, H. S. *Phys. Rev. A.* **1990**, *41*, 697.
(26) Noid, D. W.; Koszykowski, M. L.; Marcus, R. A. *J. Chem. Phys.* **1977**, *67*, 404.
(27) Sewell, T. D.; Thompson, D. L.; Levine, R. D. *J. Phys. Chem.* **1992**, *96*, 8006.
(28) Smith, R. S.; Shirts, R. B. *J. Chem. Phys.* **1988**, *89*, 2948.
(29) Davidson, N. *Statistical Mechanics*; McGraw-Hill Book Company, Inc.: New York, 1962.
(30) Liu, Y.; Lohr, L. L.; Barker, J. R. *J. Phys. Chem. B* **2005**, *109*, 8304−8309.
(31) Yardley, J. T. *Introduction to Molecular Energy Transfer*; Academic Press: New York, 1980.
(32) Lambert, J. D.; Salter, R. *Proc. R. Soc. London, A* **1959**, *253*, 277−288.
(33) Bernshtein, V.; Oref, I. *J. Phys. Chem. A.* **2001**, *105*, 10646.
(34) Linhananta, A.; Lim, K. F. *Phys. Chem. Chem. Phys.* **2000**, *2*, 1385.
(35) Logan, D. E.; Wolynes, P. G. *J. Chem. Phys.* **1990**, *93*, 4994.
(36) Lide, D. R. *CRC Handbook of Chemistry and Physics*, 81 ed.; CRC Press: Boca Raton, FL, 2000.
(37) Kiefer, J. H. Private communication.
(38) Harding. L.; Kiefer, J. H. Private communication.